



A New Dynamic Cone Penetration Test-Based Procedure for Liquefaction Triggering Assessment of Gravelly Soils

Kyle M. Rollins, M.ASCE¹; Jashod Roy, S.M.ASCE²; Adda Athanasopoulos-Zekkos, M.ASCE³; Dimitrios Zekkos, M.ASCE⁴; Sara Amoroso⁵; and Zhenzhong Cao⁶

Abstract: Developing a reliable, cost-effective liquefaction triggering procedure for characterizing the liquefaction potential of gravelly soils based on in situ penetration testing has always been a great challenge for geotechnical engineers and researchers. Typical correlations based on the standard penetration test (SPT) and the cone penetration test (CPT) are affected by large-size gravel particles, which can lead to erroneous results. The Becker Penetration Test, well known for gravelly soil characterization, is cost-prohibitive for routine projects and is not available in most of the world. With a cone diameter of 74 mm the Chinese dynamic cone penetration test (DPT) is superior to smaller penetrometers and can be economically performed with conventional drilling equipment. DPT has previously been directly correlated to field performance data, and probabilistic liquefaction resistance curves were developed based on one earthquake and geologic environment in China; however, the use of these data in other tectonic and geologic environments was not validated. In this study, 137 data points from 10 different earthquakes and different depositional environments in seven countries have been used to develop probabilistic liquefaction resistance curves. The data set was expanded by performing DPT soundings at sites around the world where gravelly soil did or did not liquefy in past earthquakes. Based on the expanded DPT database, a new set of magnitude-dependent probabilistic triggering curves has been developed using logistic regression analysis. The new triggering curves are better constrained by data and the spread between the 85% and 15% probability curves is reduced. Liquefaction resistance is shifted upward at lower DPT values. A new magnitude scaling factor (MSF) curve has also been developed specifically for gravel liquefaction which was found to be consistent with previous curves for sand. **DOI: 10.1061/(ASCE)GT.1943-5606.0002686.** © 2021 American Society of Civil Engineers.

Author keywords: Gravel; Liquefaction; Probabilistic liquefaction triggering curve; Dynamic cone penetrometer test (DPT); Magnitude scaling factor; Cyclic stress ratio.

Introduction

Assessment of the liquefaction potential of gravelly soils in a reliable, cost-effective manner remains a significant challenge for geotechnical engineers. A review of the technical literature indicates that gravelly soils have liquefied at multiple sites in at least 25 earthquakes over the past 128 years as documented in Table 1.

¹Professor, Dept. of Civil and Environmental Engineering, Brigham Young Univ., 430 Engineering Bldg., Provo, UT 84602 (corresponding author). ORCID: https://orcid.org/0000-0002-8977-6619. Email: rollinsk@byu.edu

²Ph.D. Candidate, Dept. of Civil and Environmental Engineering, Brigham Young Univ., 430 Engineering Bldg., Provo, UT 84602. Email: jashod.roy@gmail.com

³Assistant Professor, Dept. of Civil Engineering, Univ. of California, Berkeley, 760 Davis Hall, Berkeley 94720-1710, CA. Email: adda .zekkos@berkeley.edu

⁴Associate Professor, Dept. of Civil Engineering, Univ. of California, Berkeley, 760 Davis Hall, Berkeley 94720-1710, CA. ORCID: https://orcid.org/0000-0001-9907-3362. Email: zekkos@berkeley.edu

⁵Associate Professor, Dept. of Engineering and Geology, Univ. of Chieti-Pescara, Viale Pindaro, 42, Pescara 65129, Italy. Email: sara .amoroso@unich.it

⁶Professor, Guangxi Key Laboratory of Geomechanics and Geotechnical Engineering, Guilin Univ. of Technology, Guilin 541004, China. Email: iemczz@163.com

Note. This manuscript was submitted on January 8, 2021; approved on July 28, 2021; published online on September 20, 2021. Discussion period open until February 20, 2022; separate discussions must be submitted for individual papers. This paper is part of the *Journal of Geotechnical and Geoenvironmental Engineering*, © ASCE, ISSN 1090-0241.

Liquefaction assessment is particularly important for older dams that were constructed on gravelly soil foundations or with poorly compacted gravel shells before the potential for liquefaction in gravels was recognized. Likewise, many ports around the world were constructed of gravelly soils or rockfill which was believed to be immune to liquefaction. For these projects, assessing the potential for liquefaction and determining appropriate remedial measures are often multimillion-dollar decisions. These decisions involve both life-safety and regional economic issues. Over the past 10 years, gravel liquefaction has caused significant damage to ports in Greece, Chile, Ecuador, and New Zealand. Besides these large projects, gravel liquefaction must be routinely considered for a myriad of small- to medium-sized projects throughout the world.

Because undisturbed sampling and laboratory testing is not practical for most projects, innovative in situ testing procedures are being developed and evaluated for gravelly deposits (DeJong et al. 2017; Cao et al. 2013; Rollins et al. 2020). In gravelly soils, the standard penetration test (SPT) and cone penetration test (CPT) are not generally useful because of potential interference with largesized particles (Daniel et al. 2003). Although the SPT and CPT may correctly identify liquefaction in looser gravels with low penetration resistance after certain corrections are applied (Andrus 1994; Rinehart et al. 2016; Kokusho and Yoshida 1997; Seed et al. 2003), when penetration resistance increases, it becomes very difficult to determine if the observed resistance is due to the higher density of the material or an "artificial" increase associated with the large-sized particles (Cubrinovski et al. 2018; Dhakal et al. 2019, 2020). Penetration resistance may even reach refusal in cases when the soil is not particularly dense (Cao et al. 2013). To overcome this limitation, the Becker Penetration Test (BPT) has become the

© ASCE 04021141-1 J. Geotech. Geoenviron. Eng.

Table 1. Case histories involving liquefaction of gravelly soil

Earthquake	Year	M_w	Reference	
Mino-Owari, Japan	1891	7.9	Tokimatsu and Yoshimi (1983)	
San Francisco, California	1906	8.2	Youd and Hoose (1978)	
Messina, Italy	1908	7.1	Baratta (1910)	
Fukui, Japan	1948	7.3	Ishihara (1985)	
Alaska, US	1964	9.2	Coulter and Migliaccio (1966) and McCulloch and Bonilla (1970)	
Haicheng, China	1975	7.3	Wang (1984)	
Tangshan, China	1976	7.8	Wang (1984)	
Friuli, Italy	1976	6.4	Sirovich (1996a, b) and Rollins et al. (2020)	
Miyagiken-Oki, Japan	1978	7.4	Tokimatsu and Yoshimi (1983)	
Montenegro	1979	6.9	Kociu (2004)	
Borah Peak, Idaho, US	1985	6.9	Youd et al. (1985), Andrus (1994), and Harder and Seed (1986)	
Armenia	1988	6.8	Yegian et al. (1994)	
Limon, Costa Rica	1991	7.7	Franke and Rollins (2017)	
Roermond, Netherlands	1992	5.8	Maurenbrecher et al. (1995)	
Hokkaido, Japan	1993	7.8	Kokusho et al. (1995)	
Kobe, Japan	1995	7.2	Kokusho and Yoshida (1997)	
Chi-Chi, Taiwan	1999	7.8	Chu et al. (2000) and Lin et al. (2004)	
Kocaeli, Turley	1999	7.6	Bardet et al. (2000)	
Wenchuan, China	2008	7.9	Cao et al (2011, 2013)	
Tohoku, Japan	2010	9.0	Tatsuoka et al. (2017)	
Cephalonia Is., Greece	2012	6.1	Nikolaou et al. (2014) and Athanasopoulos-Zekkos et al. (2019)	
Iquique, Chile	2014	8.2	Rollins et al. (2014) and Morales et al. (2020)	
Muisne, Ecuador	2016	7.8	Lopez et al. (2018)	
Kaikoura, New Zealand	2016	7.8	Cubrinovski et al. (2017, 2018)	
Durres, Albania	2019	6.4	Pavlides et al. (2020)	

primary field test used to evaluate liquefaction resistance of gravelly soils in North American practice (Youd and Idriss 2001). Unfortunately, equipment to perform this test is not available in most other parts of the world.

The Becker Penetration Test is performed by hammering a closed-end 168-mm-diameter casing into the ground so that the penetration resistance is much less affected by particle size. However, this test is expensive, and significant uncertainty is introduced because of the need to obtain the SPT blow count using a correlation with the BPT blow count (e.g., Harder and Seed 1986; Ghafghazi et al. 2017). In addition, corrections based on the bounce chamber pressure are necessary with the interpretation procedure proposed by Harder and Seed (1986), while corrections for friction loss on the side of the BPT are necessary for other approaches (e.g., Sy 1997; DeJong et al. 2017). Although advanced instrumentation approaches such as the instrumented BPT (iBPT) promise to provide more accurate estimates of the energy that is delivered to the toe of the BPT (DeJong et al. 2017), it does not reduce the cost, complexity, or availability of the test procedure.

As another alternative for gravelly soils, Chinese engineers in the Chengdu region, faced with widespread gravel deposits, developed a dynamic cone penetrometer (DPT) with a 74-mm-diameter cone for site characterization (Chinese Design Code 2001). The methodology is a large-size implementation of the lightweight dynamic cone penetrometer that is used extensively for assessment of compaction of soils in pavement applications (ASTM 2018) and different cone geometries are also known as dynamic probing in Europe (BSI 2012). In the Chinese version of the DPT used in this study, the cone is driven continuously with a 120 kg hammer dropped from one meter and is capable of penetrating medium to dense gravel and cobbles. DPT soundings can be easily performed with conventional SPT drilling rigs or even simple tripod systems, making it viable worldwide. In contrast to the straight sides of the BPT, the cone tip tapers back to a 60-mm drill rod to reduce rod friction. Chinese experience indicates that skin friction on the drill rods is relatively minor for depths less than about 20 m (Cao et al. 2013).

At 74 mm, the DPT diameter is 50% larger than the SPT and 110% larger than a standard 10 cm² CPT; however, it is still 55% smaller than the BPT. Although the BPT provides the largest diameter to particle size ratio of all tests due to its larger size, the DPT is superior to the SPT and the CPT, and it could be a reasonable solution in many cases depending on the gravel size and percentage.

Based on field case histories of gravel liquefaction in the M_w 7.9 Wenchuan earthquake, Cao et al. (2013) developed probabilistic liquefaction triggering curves for gravels based on the DPT blow count as shown in Fig. 1(a). However, these curves are based on relatively few data points from one earthquake and a geologic profile consisting of a loose alluvial fan gravel layers overlain by a clay surface layer typically 2- to 4-m thick (Cao et al. 2013). Because of the limited number of data points and the possibility of false negatives (sites where liquefaction may have occurred but did not produce surface manifestation), the individual triggering curves (85% to 15%) are spread apart. In contrast, probabilistic liquefaction triggering curves for sands based on CPT (Boulanger and Idriss 2015) shown in Fig. 1(b) have more closely grouped probability curves because of their larger data set.

In addition, the Cao et al. (2013) triggering curves were developed for a single event of $M_{\rm w}$ 7.9 without incorporating any correction to the seismic demand by using a magnitude scaling factor (MSF). Thus, the applicability of these curves would become questionable for evaluating the liquefaction potential of gravelly soils for other seismic events of different magnitude. Although existing MSF models developed for sand liquefaction (Youd and Idriss 2001) can be used, it is unclear whether they are appropriate for gravel liquefaction using the DPT. Therefore, it becomes crucial to add more case histories to the DPT database for different earthquake magnitudes and from different geologic settings to develop an improved DPT-based liquefaction triggering procedure and a gravel-based MSF curve.

Hence, in the present study, an expanded set of DPT data consisting of 137 sites for 10 earthquakes in seven countries has been collected where gravel liquefaction did or did not occur. These data

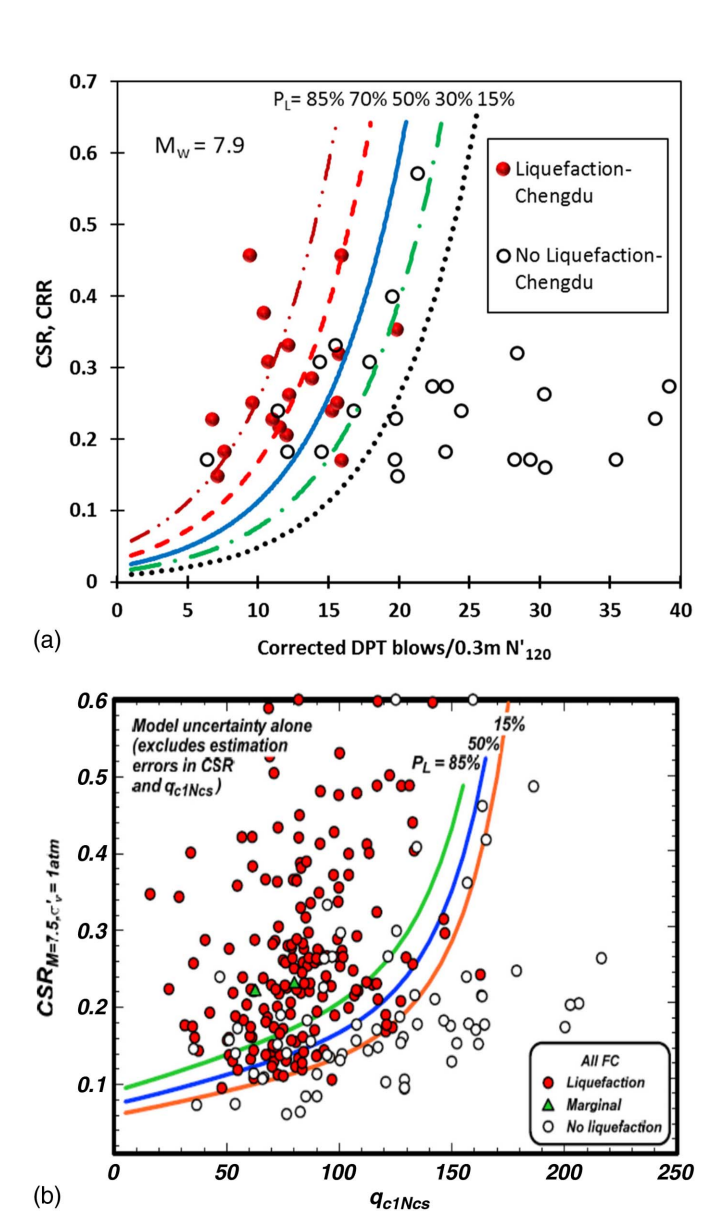


Fig. 1. Comparison of (a) DPT-based probabilistic liquefaction triggering curves for gravel (reproduced from Cao et al. 2013 © ASCE); and (b) CPT-based probabilistic liquefaction triggering curves for sand (reproduced from Boulanger and Idriss 2015 © ASCE).

points, including the 47 data points originally collected by Cao et al. (2013), have been used to develop an improved set of probabilistic triggering curves for gravelly soil by logistic regression analysis. The improved triggering equations include the earthquake magnitude as an independent variable which led to the development of a new MSF model exclusively for gravelly soils based on DPT. Details of the development of this improved liquefaction triggering procedure along with a brief background of the liquefaction evaluation framework based on the Chinese DPT are provided in this paper.

Dynamic Cone Penetration (DPT) Test Corrected Blow Count

The DPT blow count, N_{120} , represents the number of hammer blows to drive the penetrometer 30 cm deep with a 120 kg hammer dropped from a height of 1 m. As standardized by the Chinese

Design Code (2001), raw blow counts are typically reported at every 10 cm of penetration but are multiplied by three to get the equivalent N_{120} for 30 cm of penetration to maintain consistency with the SPT drive length as well as preserve the 10-cm detail in the penetration profile (Cao et al. 2013). The use of the 10-cm interval provides additional resolution of potential layering relative to a 30-cm interval, but is large enough to minimize large fluctuations that may not be representative of the profile.

Based on 1,200 hammer energy measurements, Cao et al. (2012) found that the Chinese DPT provided an average of 89% of the theoretical hammer free-fall energy. Since the energy delivered by a given hammer ($E_{\rm Hammer}$) may be different than the energy transferred by a Chinese DPT hammer ($E_{\rm Chinese\ DPT}$), it may be necessary to correct the measured blow count. In this study, the correction was made using the simple linear reduction suggested by Seed et al. (1985) for SPT testing:

$$N_{120} = N_{\text{Hammer.}}(E_{\text{Hammer}}/E_{\text{Chinese DPT}})$$
 (1)

where $N_{\rm Hammer}$ is the number of blows per 0.3 m of penetration obtained with a hammer transferring an energy of $E_{\rm Hammer}$ to the drill rods. Although this energy correction equation was developed for sand, the correction factors were generally found to be appropriate based on tests in gravelly soils in Friuli, Italy (Rollins et al. 2020), Alaska (Rollins et al. 2020), and Idaho (Talbot 2018). Therefore, it appears that the energy correction factor is primarily a function of the energy of the hammer rather than the material it penetrates. However, additional data would be desirable for denser gravels to confirm this result.

In addition, Cao et al. (2013) recommend an overburden correction factor, C_N , to obtain the normalized N'_{120} value using the equation

$$N_{120}' = N_{120}C_N \tag{2}$$

where

$$C_N = (100/\sigma'_{vo})^{0.5} \le 1.7$$
 (3)

and σ'_{vo} is the initial vertical effective stress in kN/m². In the current study, a limiting value of 1.7 was added to be consistent with the C_N used to correct penetration resistance from other in situ tests (Youd and Idriss 2001). It should be noted that Eq. (3), originally developed by Liao and Whitman (1986), was recommended for sandy soils with a wide range of gradations and relative densities. Hence, the use of Eq. (3) to estimate C_N for gravelly soil is a reasonable approximation when the gravelly deposits contain a considerable percentage of sand as is often observed for liquefiable gravels. More recent liquefaction triggering methods (Boulanger and Idriss 2014; Idriss and Boulanger 2008) correlate C_N with both σ'_v and relative density (D_r) , obtained from in situ tests. Calibration chamber tests with the DPT in gravels would be necessary to establish these relationships for gravels, similar to those performed by Gibbs and Holtz (1957) for sands with the SPT. Although this would certainly be valuable, it is beyond the scope of this paper.

DPT-Based Case History Data

As a part of this study, the gravel liquefaction case history database has been considerably expanded by performing DPT tests at sites around the world where gravelly soil liquefaction has been identified (Table 1). The sites where features of gravel liquefaction (e.g., surface ejecta of gravelly soils, lateral spreading, settlement manifestation, etc.) were observed have been considered as liquefaction points, and the DPTs have been conducted within a couple meters

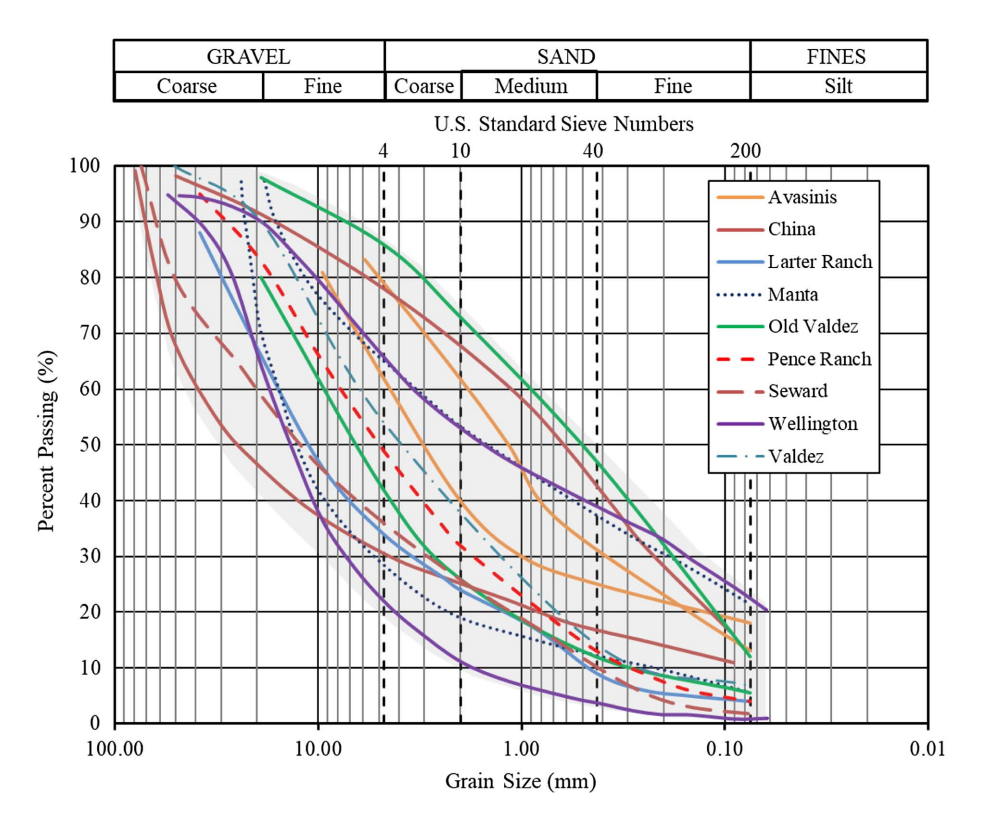


Fig. 2. Range of grain size distribution curves for liquefiable gravelly soil based on the collected case history database.

of the locations of liquefaction manifestation to measure the representative blow counts of the liquefiable strata. In addition, DPT tests were performed at sites where no liquefaction manifestation was observed within 1,000 m or more despite having loose to dense gravel layers. These no-liquefaction points provide an important constraint on the triggering curves. In some cases, these points were for the same sites identified in Table 1, but for smaller earthquakes that did not produce liquefaction effects. In other cases, these sites were carefully selected for DPT testing to fill gaps in the data set. In these no-liquefaction cases, there may be some false negative points (Boulanger and Idriss 2014; Cao et al. 2013) where liquefaction might have taken place, but no surface manifestation was observed. This could be due to the presence of a thick impermeable clay layer on top of the gravelly strata which could prevent the gravelly ejecta from moving to the surface or due to the weight and size of gravel particles relative to crack width available for escape. These issues can not be conclusively addressed by mere site investigation in the present study and remain a source of uncertainty in the development of the triggering curves.

Salient information for each individual case history along with the relevant references are summarized in Table S1. Additional details for each site, including the soil strata and grain size distribution of the liquefied gravelly soils, can be found in the respective references listed in the table. A summary of the range of gradation curves for the sites is shown in Fig. 2, which indicates the overall range of the particle size distribution of the potentially liquefiable gravelly deposits. Fig. 2 shows that the gravelly deposits for the sites contain 20% to 70% gravel according to the 4.75-mm particle size criterion. This newly collected data set has been added to the existing Chinese database to develop a new set of triggering curves. As noted previously, the Cao et al. (2013) data set consisted of 47 case histories (19 liquefaction sites and 28 nonliquefaction sites) in alluvial deposits resulting from the M_w 7.9 Wenchuan, China earthquake. In contrast, the expanded data set consists of 137 case

histories (80 liquefaction sites and 57 nonliquefaction sites) resulting from 10 separate earthquakes in seven countries. This collection of data represents a 190% increase in the number of case histories.

Although most of the new data points come from outside of China, there are also 15 additional case histories from Chengdu, China (Cao et al. 2019) and Tangshan, China in addition to the original 47-point data set (Cao et al. 2013). The distribution of data collected from different countries is shown by the bar chart in Fig. 3. Although China provides the most data points, the majority of data points are now from countries outside of China. The gravel layers were both manufactured fills at ports and dams, as well as natural

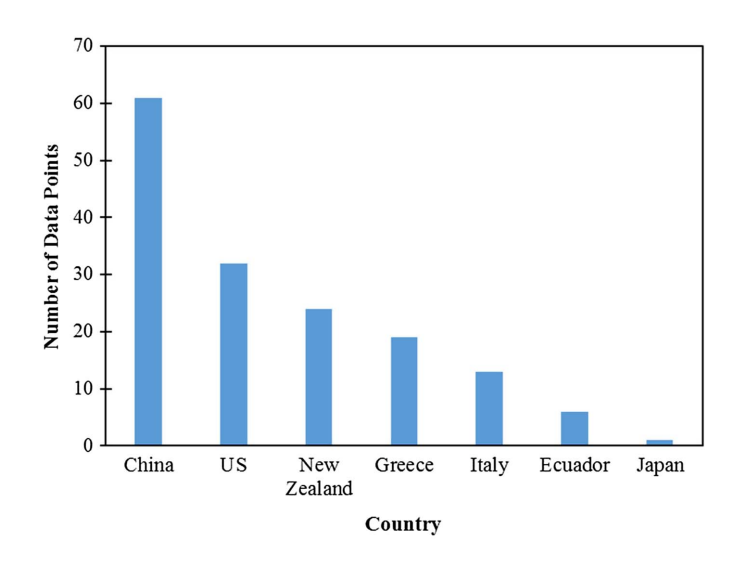


Fig. 3. Distribution of countries with gravel liquefaction case histories for the DPT data set.

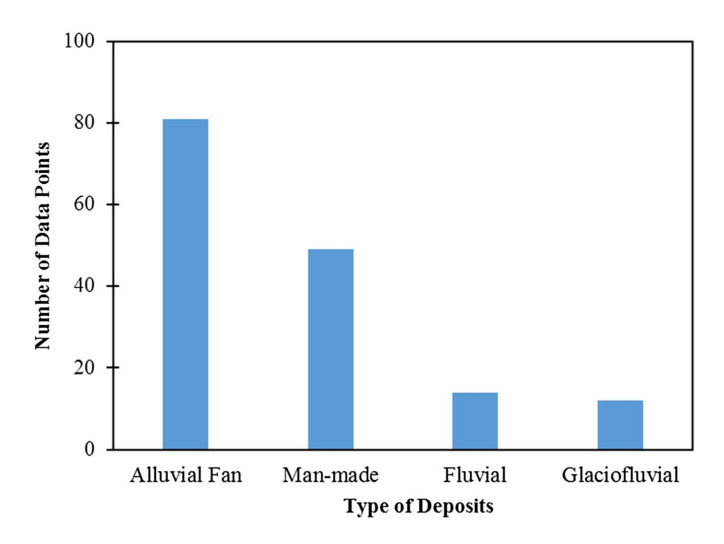


Fig. 4. Distribution of deposition type for gravel liquefaction case history data set.

deposits from alluvial fans, glacial outwash, and fluvial processes. Fig. 4 provides a bar chart to graphically illustrate the distribution of different types of soil deposits represented in the gravel lique-faction case histories. This figure depicts that the largest number of gravel liquefaction incidents took place in the alluvial deposits and manufactured fills, whereas glaciofluvial and fluvial deposits represent a smaller number of the gravel liquefaction case histories.

At most sites, DPT soundings were performed using the standard Chinese hammer energy (120 kg weight and 1 m drop) or by performing companion DPT tests with both the Chinese hammer energy and the SPT hammer energy (63.5 kg weight and 0.76 m drop). The hammer energy transferred to the drill rods was measured by a pile driving analyzer (PDA) device at each respective location. After correction for hammer energy using Eq. (1), results from the two hammers were found to provide comparable N_{120} value over an average interval (Rollins et al. 2020, 2018) for N_{120} values less than about 25. At sites in New Zealand and Greece, DPT tests were performed using the SPT hammer energy only along with energy transfer measurements. At all sites, the measured blow counts have been calibrated to the Chinese hammer energy using Eq. (1) to obtain N_{120} , and these values have then been converted to N'_{120} by applying the overburden correction factor given by Eq. (2).

The cyclic stress ratio (CSR) has been obtained using the simplified equation

$$CSR = 0.65(a_{\text{max}}/g)(\sigma_{vo}/\sigma'_{vo})r_d \tag{4}$$

originally developed by Seed and Idriss (1971) where a_{max} is the peak ground acceleration, σ_{vo} is the initial vertical total stress, σ'_{vo} is the initial vertical effective stress, and r_d is a depth reduction factor as defined by Youd and Idriss (2001).

The peak ground acceleration (PGA; a_{max}) for nearly every location was obtained from nearby strong ground motion stations (SGMS) or from USGS ShakeMaps (Worden et al. 2010) where necessary as employed by Idriss and Boulanger (2008) for their CPT database. As per the references given in Table S1, the PGAs at the sites of Manta, Japan, Wellington, Lixouri, and Argostoli were obtained from the nearby SGMS records. The PGAs at the Chengdu Plain in China were estimated from contour maps developed from the nearby SGMS records. At the sites in Italy, the SGMS were located in the vicinity of Avasinis but not near to the liquefied areas. Hence, the estimated PGAs from the SGMS were verified with the

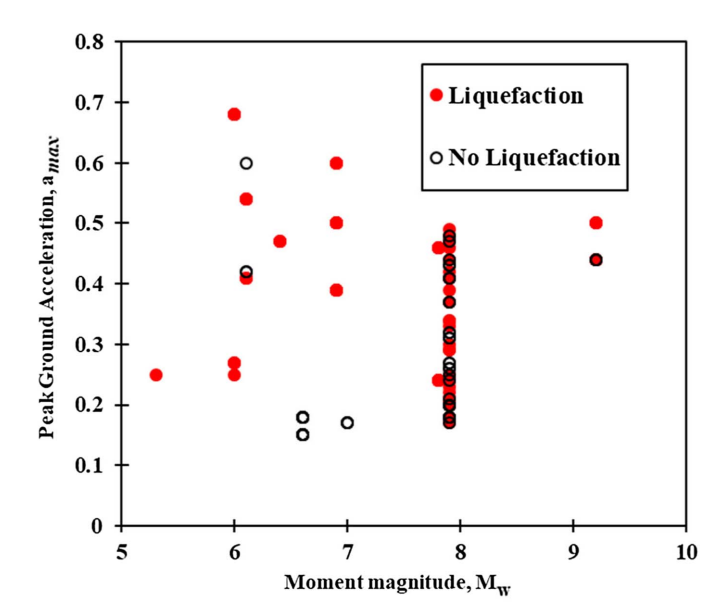


Fig. 5. Distribution of earthquake moment magnitude (M_w) and corresponding peak ground acceleration (a_{max}) for the expanded data set.

results of ground motion prediction equation (GMPE) (Bindi et al. 2011) and USGS ShakeMap estimations as reported in Rollins et al. (2020). At the sites in Alaska, PGAs were obtained from the USGS ShakeMaps owing to the absence of SGMS records. PGAs at sites in Idaho during the Borah Peak earthquake were based on ground motion prediction equations. Overall, 85% of the PGA data are directly based on SGMS records, 13% are from USGS ShakeMaps, and the remaining 2% come from GMPE. Although estimation of PGA is an important source of uncertainty in liquefaction assessment, the fact that a large percentage of PGAs for this study are based on measured values tends to moderate the uncertainty. Besides CSR, the moment magnitude (M_w) has been considered as another independent seismic variable for obtaining the liquefaction potential of gravelly soils. Values of M_w are also given in Table S1 based on the references. The distribution of M_w versus a_{max} for all data points is plotted in Fig. 5. The data set contains a wide distribution of M_w values ranging from 5.3 to 9.2 as well as a_{max} ranging from 0.17g to 0.6g. Some points on the plot represent multiple sites in the database.

Data Interpretation for Selection of Critical Layer

Based on the plots of N'_{120} versus depth and CSR versus depth, the critical layer for each location was selected as the layer that was most likely to trigger and manifest liquefaction at the ground surface (Seed et al. 2003; Cubrinovski et al. 2018). Typically, this was the gravelly layer corresponding to the lowest average N'_{120} values below the water table relative to the CSR. Cohesive layers were excluded from consideration. The critical layer was selected having a thickness of about one meter or more to provide a representative average N'_{120} value which is less affected by thin peaks or troughs (Boulanger and Idriss 2014). As an example, a typical soil profile from Alaska with DPT resistance (N'_{120}) and probability of liquefaction profile along the depth and the corresponding critical layer is shown in Fig. 6 to illustrate the critical layer selection method. The values of all the parameters (e.g., N'_{120} , CSR, etc.) for every location, shown in Table S1, have been obtained based on the critical layer.

The distribution of the critical layer depth and corresponding DPT N'_{120} for all the data points is illustrated in Fig. 7. The plot

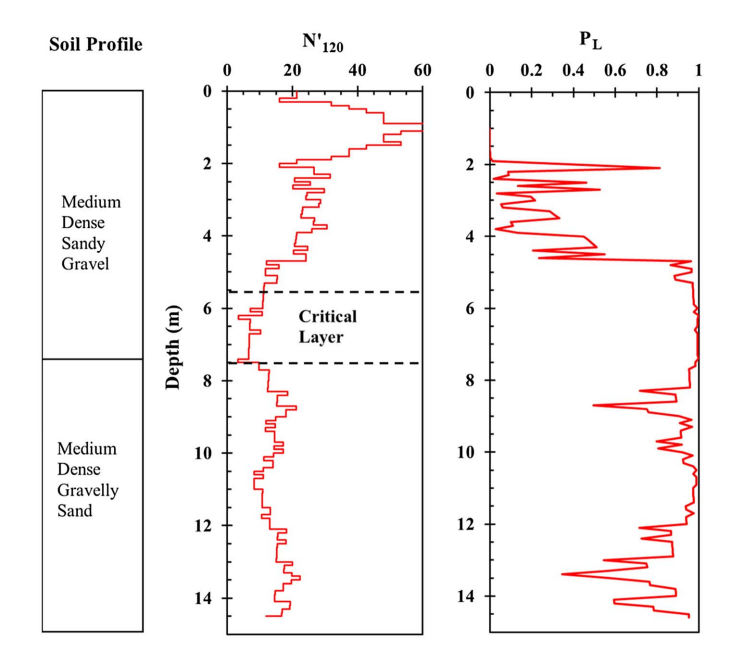


Fig. 6. Representative profiles of DPT blow count (N'_{120}) and probability of liquefaction (P_L) from Old Valdez, Alaska, with selected critical liquefaction layer.

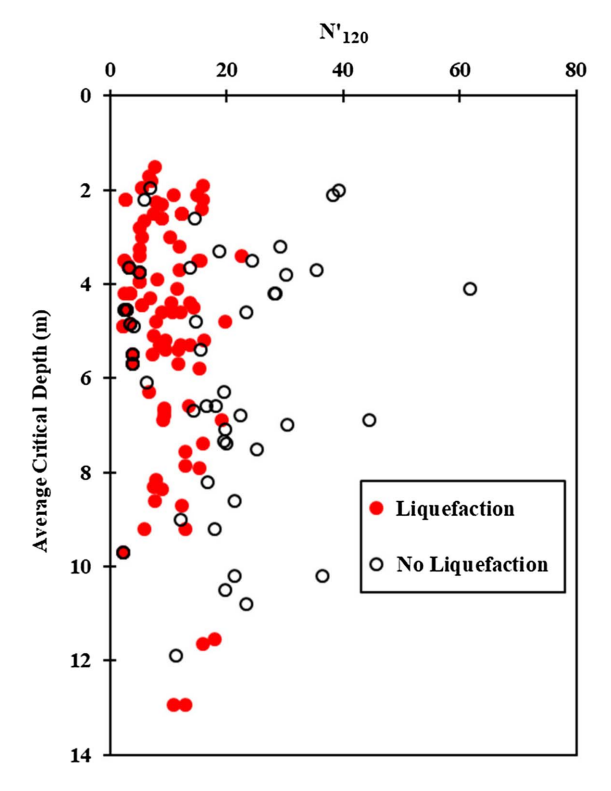


Fig. 7. Distribution of critical layer depth and corresponding corrected DPT blow count (N'_{120}) for the expanded gravel liquefaction case history data set.

shows that all the critical gravel layers are restricted within a depth of 14 m and N'_{120} values for the critical liquefied layers are typically less than about 20. This depth range is consistent with previous investigations. For example, Youd and Idriss (2001) indicate that most of the empirical SPT liquefaction data were for layers less

than 15 m in depth. Likewise, Cubrinovski et al. (2017) noted that "in the updated database of liquefaction manifestation case histories of Boulanger and Idriss (2014), out of over 250 CPT-based case histories there is only one case in which the depth of the critical zone (liquefaction) was greater than 10 m." On the other hand, the N'_{120} values for no-liquefaction points are greater than 20 for larger CSRs but can be less than 20 for smaller CSRs.

Besides penetration resistance and earthquake variables, there are other significant parameters, such as fines content, plasticity index, sand content, particle angularity, hydraulic conductivity, and thickness of the impermeable clay layer overlying the gravelly strata, that may also play a role in governing the liquefaction potential of some gravelly soil sites. For example, cyclic simple shear laboratory testing on uniform gravels and gravel-sand mixes using both rounded and angular particles have shown an increase in liquefaction resistance with particle angularity (Hubler et al. 2017, 2018).

Fines content has often been included as an independent variable in SPT- or CPT-based correlations for evaluating liquefaction potential of sands (Youd and Idriss 2001). Unfortunately, in the present study on gravelly soils, there is insufficient data for each site to statistically identify the influence of fines content on liquefaction resistance. As noted by Seed et al. (1976), gravels with a hydraulic conductivity higher than 0.3 cm/sec are unlikely to liquefy because of rapid drainage. However, the presence of an impermeable cap layer of clay or concrete, which is present in many of the case histories (e.g., Cao et al. 2013; Yegian et al. 1994; Rollins et al. 2020; Chen et al. 2018) may inhibit drainage during an earthquake.

Even in cases for which an impervious cap is not present, soils classifying as gravels according to the Unified Soil Classification System could still have hydraulic conductivities low enough to generate excess pore pressure in an earthquake. For example, She et al. (2006) found that a sand content of 30% typically reduced the hydraulic conductivity of gravel-sand mixtures to that of the sand. In addition, DeJong et al. (2016) report that the permeability of sandy gravel mixtures is controlled by the D_{10} size of the sand sized particles, as recognized by Hazen (1911), which enables excess pore pressure to be generated. A brief review of the average gradation curves for the present data set, as shown in Fig. 2, indicates that most gravelly sites have a high enough sand content and a small enough D_{10} to reduce the hydraulic conductivity below the threshold for liquefaction during earthquake shaking. Therefore, in these cases it would not be necessary to have an impermeable layer to restrict water flow and induce liquefaction. However, the amount of data on the hydraulic conductivity and the controlling parameters are still not sufficient to be included in the regression analysis to develop a clear mathematical perspective about the significance of these parameters in governing the liquefaction phenomena.

Liquefaction Evaluation by Cao et al. (2013) Triggering Procedure

The collected database given in Table S1 provides a good opportunity to evaluate the performance of the DPT-based triggering curves developed by Cao et al. (2013) for predicting the liquefaction potential of gravelly soils. In this context, it should be noted that these correlations and the corresponding triggering curves were developed specifically for a M_w 7.9 earthquake event. Hence, while performing the liquefaction evaluation for the present data set with a variety of magnitudes, the set of triggering curves originally developed by Cao et al. (2013) have been modified to the M_w 7.5 earthquake reference standard using MSF factors given by the following equation suggested by (Youd and Idriss 2001).

$$MSF = 10^{2.24} / M_w^{2.56} \tag{5}$$

Hence, the modified form of the equation for obtaining the probability of liquefaction (P_L) is given by

$$P_L = \frac{1}{1 + \exp[-8.51 + 0.36N'_{120} - 2.26\ln(\text{CSR}_{M=7.5})]}$$
 (6)

where, $CSR_{M=7.5}$ is obtained by the equation

$$CSR_{M=7.5} = CSR/MSF \tag{7}$$

Rearranging Eq. (6), the cyclic resistance ratio (CRR) at M_w 7.5 can be expressed as:

$$CRR_{M=7.5} = \exp\left[\frac{0.356N'_{120} - 8.51 - \ln\left(\frac{1 - P_L}{P_L}\right)}{2.26}\right]$$
(8)

Using Eq. (8), a modified set of triggering curves have been obtained for 15%, 30%, 50%, 70%, and 85% probability of lique-faction. In addition, the CSRs of all the data points having different earthquake magnitudes have also been converted to M_w 7.5 using Eq. (7). These corrected CSRs and their corresponding N_{120}' values have been plotted along with the modified triggering curves, as shown in Fig. 8, to facilitate proper comparison within the same framework.

Fig. 8 indicates that most of the newly added liquefaction points are generally evaluated satisfactorily by the Cao et al. (2013) triggering curves with probabilities of liquefaction greater than 50%. In addition, the no-liquefaction points from L'Aquila also fall below the 50% probability of liquefaction curve. In contrast, the no-liquefaction points from the Port of Wellington in the M_w 6.6 Cook

Strait and M_w 6.6 Lake Grassmere earthquakes and the Port of Argostoli in the 1983 M_w 7.0 Cephalonia Earthquake plot much higher than the Cao et al. (2013) triggering curves. In other words, these sites are interpreted as liquefied, which is inconsistent with the actual case histories. This result indicates that the triggering curves need to shift upward at lower N'_{120} values. These observations support the need for a new set of improved triggering curves, based on the expanded data set, to provide a better assessment of liquefaction observed in the field case histories, and possibly reduce the spread in the triggering curves from 15% to 85% since false negatives become a smaller percentage of the total data set.

Development of New Probabilistic Triggering Curves

In this study, a logistic regression analysis (Liao et al. 1988; Youd and Noble 1997; Cao et al. 2013) has been performed on the entire data set given in Table S1 to obtain a new set of triggering curves. Most of these data points represent a single DPT hole located 100 m or more from another; however, some points represent the average of multiple DPT holes when located within about 50 m of each other because the penetration resistance of closely spaced boreholes would represent similar soil profiles instead of representing different soil strata.

Unlike the correlation of Cao et al. (2013) which involved only one earthquake event, in performing the logistic regression analysis in the present study, the moment magnitude M_w of each data point has been considered as an explanatory variable in addition to the DPT blow count (N'_{120}) and the natural log of the cyclic stress ratio [ln(CSR)]. While computing the CSR, the r_d value in Eq. (4) was updated to include the effect of magnitude on the variation of r_d with depth using the equation

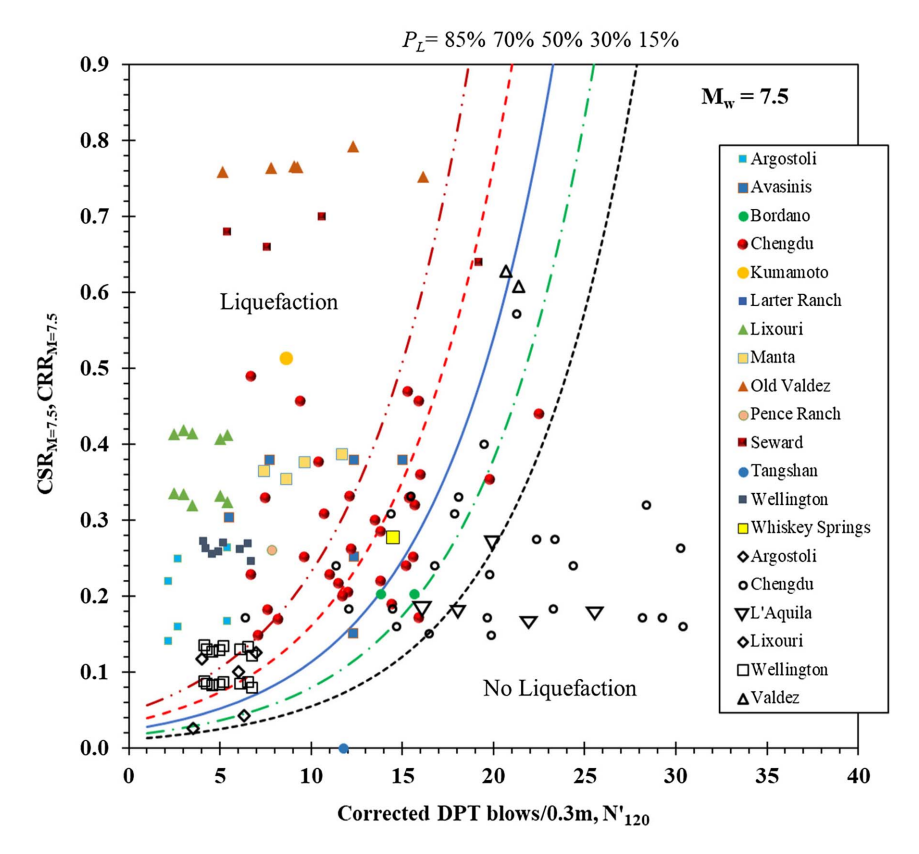


Fig. 8. Comparison of $CSR-N'_{120}$ points for all collected data with probabilistic liquefaction triggering curves developed by Cao et al. (2013). Symbols for liquefied sites are filled, while symbols for nonliquefied sites are not filled.

$$r_d = e^{\left[\alpha(z) + \beta(z)M_w\right]} \tag{9}$$

where

$$\alpha(z) = -1.012 - 1.126 \sin\left(\frac{z}{11.73} + 5.133\right) \tag{10}$$

$$\beta(z) = 0.106 + 0.118 \sin\left(\frac{z}{11.28} + 5.142\right) \tag{11}$$

and z is the depth in meters, based on the work by Golesorkhi (1989) and Idriss (1999).

Regression Model

According to the logistic regression analysis method, the probability of liquefaction occurring (P_L) is expressed by the general equation

$$P_L(\theta, X) = \frac{1}{1 + \exp(\theta_1 X_1 + \theta_2 X_2 + \dots + \theta_n X_n)}$$
 (12)

where the series of Xs represents the soil and the earthquake parameters on which the liquefaction potential depends. In this case, these variables are N_{120}' , M_w , and ln(CSR) along with various combinations of these primary variables. The vectors θ are the model coefficients that need to be estimated to define the function of gravel liquefaction potential. Typically, these coefficients are obtained by the maximum likelihood method. The likelihood function can be expressed as

$$L(\theta, X) = \prod [P_L(\theta, X)]^n [1 - P_L(\theta, X)]^{m-n}$$
 (13)

where m = the total number of data points in the sample; n = the total number of liquefied sites (i.e., m - n = total number of non-liquefied sites). To maximize this likelihood function, the following condition should be satisfied;

$$\frac{\partial L(\theta, X)}{\partial \theta_i} = 0; \quad i = 1, 2, \dots, n$$
 (14)

By satisfying Eq. (14), *n* number of equations can be obtained that need to be solved to estimate the coefficients of the model parameters. However, these procedures require rather tedious and extensive numerical programming, which was easily accomplished using the variable selection procedure (Youd and Noble 1997) with the JMP Pro version 13 software package.

A brief description of the regression analysis associated with the stepwise variable selection procedure is provided in this section.

Step 1: First, a set of explanatory variables was defined by combining soil resistance and earthquake parameters in different forms. Hence, the probability of liquefaction can be expressed as a function of these variables as given by Eq. (12) and the first cycle of regression is performed on this set to estimate the model parameters. The explanatory variables included in the first set were $[N'_{120}, N'^2_{120}, N'^3_{120}, N'^4_{120}, M_w, \ln(\text{CSR})]$ and different combinations of these basic variables such as $M_w \ln(\text{CSR}), M_w N'_{120}$, and $N'_{120} \ln(\text{CSR})$.

Step 2: After the first cycle was completed, the chi-square test and P-values (the probability that the level of prediction of the model would decrease if the explanatory variable provided zero contribution to the model) were checked for the estimated parameters of all the variables. The variable having the maximum *P*-value and minimum chi-square were eliminated from the set of explanatory variables because they provide the minimum contribution to the predictive model. Hence, a new regression analysis is performed based on the new set of variables.

Table 2. Results of model parameter estimates from logistic regression analysis

Candidate variables	Parameter estimates $(p < 0.05)$							
	Trial 1	Trial 2	Trial 3	Trial 4	Trial 5	Trial 6		
N'_{120}	0.279	_	_	_	-0.588	_		
$(N_{120}')^2$	_	0.0153	_	_	0.0406	-0.0334		
$(N_{120}')^3$	_	_	0.0009	_	_	0.0033		
$(N_{120}')^4$	_	_	_	0.00004	_	-0.00004		
M_w	-1.375	-1.497	-1.45	-1.44	-1.249	-1.318		
ln(CSR)	-4.568	-5.58	-5.55	-5.77	-5.963	-5.523		

Step 3: Steps 1 and 2 are repeated iteratively and the insignificant variables are excluded from the prediction model based on the chi-square test and probability values. These cycles of regression are performed until the probability values of the explanatory variables remaining in the model become less than 0.05.

Analysis Results and Discussion

Following Steps 1–3, various forms of equations which include lower to higher degrees of polynomials in N'_{120} , M_w , and ln (CSR) were obtained, and the coefficient estimates for these different forms are summarized in Table 2. The set of results shows that no combination of the basic explanatory variables was found to be statistically significant. Although all of the solutions given in Table 2 are statistically admissible, they do not perform equally well in separating the liquefaction and no-liquefaction points in a realistic manner.

The formulation of CRR obtained from the solution of Trial 1 as given in Table 2 produces a set of triggering curves which become unrealistically sloped and that widen with blow count because it is a function of only a first-order polynomial in N'_{120} . The triggering curves obtained from the solution of Trials 2, and 5 which contain the N'_{120} polynomials up to second order are much improved compared to the first-order solution, but they still show a considerable slope at the upper end of the curve and do not satisfactorily evaluate the liquefaction potential of some no-liquefaction points. On the other hand, the solutions having N'_{120} polynomials up to fourth order (Trials 4 and 6) make the triggering curves too steep and vertical from the middle to high range of CSR which is unrealistic and does not properly evaluate some no-liquefaction points. Hence, by judging the performance of all these curves for the given data set, the Trial 3 solution based on a third-order polynomial $(N'_{120})^3$ was determined to be the most realistic way of determining the liquefaction potential of the existing points in a reliable manner. Therefore, the recommended equation for obtaining the probability of liquefaction from this updated regression analysis is given by

$$P_L = \frac{1}{1 + \exp[0.0008N_{120}^{\prime 3} - 1.32Mw - 5.2\ln(\text{CSR})]}$$
 (15)

After rearrangement of Eq. (15), the revised CSR can be written in the following form:

$$CRR = \exp\left[\frac{0.0008N_{120}^{3} - 1.32M_w - \ln\left(\frac{1 - P_L}{P_L}\right)}{5.2}\right]$$
 (16)

Substituting $M_w = 7.5$ and P_L for various probabilities of liquefaction, the relationship between N'_{120} and CSR can be obtained.

Development of Magnitude Scaling Factor

As shown in Fig. 8, the original CSRs for all the data points at various M_w values were converted to CSRs at M_w 7.5 using Eq. (5), the lower-bound MSF curve recommended by the National Center for Earthquake Engineering Research/National Science Foundation (NCEER/NSF) workshop (Youd and Idriss 2001). This equation was primarily developed for liquefaction of sand and could also be part of the reason that the liquefaction potential of several case histories was not correctly evaluated using the Cao et al. (2013) triggering curves. However, in the newly developed regression model, the moment magnitude, M_w , has been kept as an independent variable as shown in Eqs. (15) and (16). Therefore, as a part of the present study, we have developed a new MSF model specifically for gravelly soils that may help improve liquefaction evaluation at some gravel sites, although more data from other earthquakes would be desirable.

To obtain the MSF, CSR values were first obtained from Eq. (16) for M_w 5.5 through 9 with an increment of 0.5 keeping N_{120}' and P_L constant. Then the CSRs for different magnitudes were divided by the CSR at $M_w = 7.5$ to obtain the magnitude scaling factor. The same process was then repeated by substituting different values of N_{120}' and P_L in Eq. (16) to obtain the variation of MSF with these variables. But notably, the MSF pattern did not show any significant variation with the DPT blow count (N_{120}') and the probability of liquefaction (P_L). Based on this analysis, the MSF can be computed as a function of magnitude with the best-fit exponential equation:

$$MSF = 7.258 \exp(-0.264M_w) \tag{17}$$

This MSF curve is plotted and compared with several other MSF curves (Seed and Idriss 1982; Andrus and Stokoe 1997; Youd and Idriss 2001; Idriss and Boulanger 2008; Kayen et al. 2013) in Fig. 9. It can be observed that the MSF model developed for gravelly soil falls about midway between the lower-bound curve recommended by the NCEER/NSF liquefaction workshop (Youd and Idriss 2001) and the original MSF curve developed by Seed and Idriss (1982) for sand. In addition, the MSF curve from this study is nearly identical with the curve proposed by Idriss and

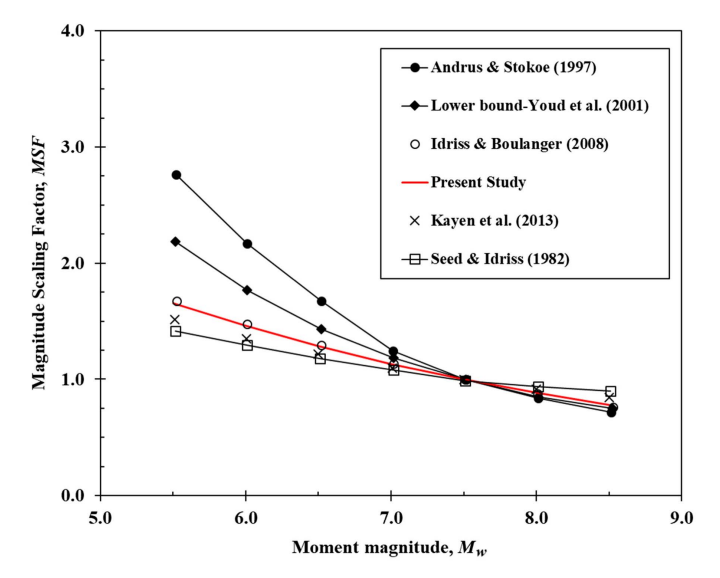


Fig. 9. Comparison of magnitude scaling factor (MSF) from logistical regression analysis of gravel liquefaction case histories in this study along with MSF curves proposed previously for sand.

Boulanger (2008) for sand. Hence, the proposed model for gravel appears to be reasonably consistent with existing MSF curves for sands.

Based on this MSF model Eq. (17), the CSRs for all the case history data points have been converted to CSRs at $M_w = 7.5$ and plotted with the newly developed triggering curves obtained by Eq. (16) as shown in Fig. 10. Fig. 10 shows that all the data points have been slightly relocated and the liquefaction potential of the marginal points are evaluated relatively better compared to Fig. 8. This is particularly true for the case histories at the port of Wellington in New Zealand and at the port of Argostoli in Cephalonia where liquefaction and no-liquefaction data points are now located on the correct side of the 50% probability curve. In addition, the larger data set and additional no-liquefaction data points have reduced the range of the probability of liquefaction curves. Therefore, the newly developed triggering procedure in association with the MSF model provides better estimates of the liquefaction resistance for gravelly soil deposits than previous approaches.

Discussion on the New Triggering Curves in Comparison to the Cao et al. (2013) Triggering Curves

The new probabilistic triggering curves with liquefaction probabilities of 15% to 85% are plotted in Fig. 11 with solid lines along with similar curves originally developed by Cao et al. (2013) with dashed lines to draw a distinct comparison between the two triggering procedures. The new set of triggering curves intercept the CRR axis at values between about 0.1 to 0.2, which provides better agreement with the observed data points for the lower range of DPT N'_{120} values compared to the Cao et al. (2013) curves which intercept the CRR axis near the origin. The higher CRR intercept is more typical of that observed for SPT (Youd and Idriss 2001) and CPT (Boulanger and Idriss 2014) curves. In fact, it can be seen from Fig. 10 that the points from the Port of Wellington where liquefaction did not take place during the Cook Strait and Lake Grassmere earthquakes (both $M_w = 6.6$) in 2013 and the noliquefaction points from Argostoli have had a significant effect in constraining the lower branch of the triggering curves to move upwards. Likewise, the triggering curves at the higher range of N'_{120} values have been tightened and steepened relative to the curves developed by Cao et al. (2013) as a result of the no-liquefaction data points from Valdez and L'Aquila. Nevertheless, it can be observed from Fig. 10 that one point from Valdez where liquefaction did not occur during the 1964 Alaska earthquake is correctly evaluated because it falls just below the 30% line, but the other no-liquefaction point falls very close to the 50% line, still showing inconsistent evaluation of performance. Additional data points would certainly be desirable to better define the shape of the curve in this region.

In the middle range of the curve, a few no-liquefaction points from the Chengdu plain fall above the 70% triggering curve and some liquefaction points from the same region fall below the 30% triggering curve. These points may belong to the false negative or false positive categories, as explained previously, leading to inconsistent evaluation of the actual incident. Due to the presence of these points, the set of triggering curves develops a slightly sloped shape above an N'_{120} value of 17 such that a number of no-liquefaction points from Chengdu, Argostoli, and L'Aquila fall marginally on the 30% triggering curve. This set of points might be governed by some other site parameters such as the permeability of the soil strata, presence of impermeable clay layer above the gravelly strata, or fines content, which have not been included in the present regression analysis due to a lack of data. Hence, the discrepancy of

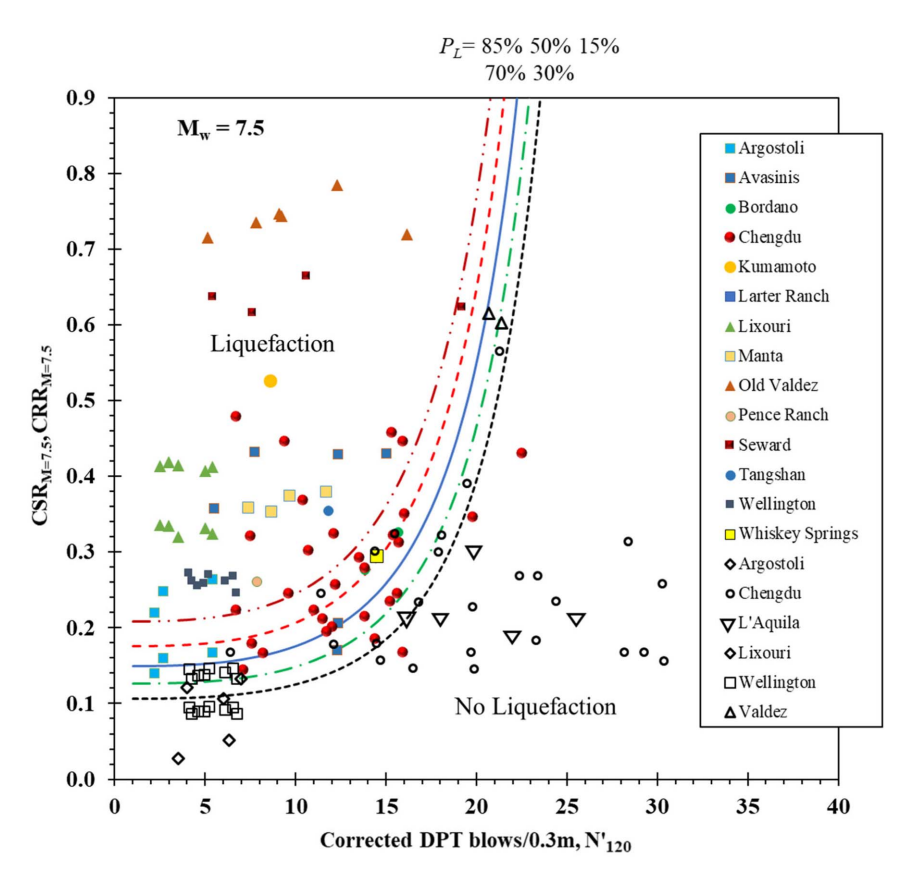


Fig. 10. New probabilistic liquefaction triggering curves from this study using all available data points adjusted to M_w 7.5 with new magnitude scaling factor (MSF). Symbols for liquefied sites are filled, while symbols for nonliquefied sites are not filled.

these points remains a source of uncertainty in the overall liquefaction triggering formulation.

As shown in Fig. 11, for N'_{120} values above 15, the $P_L = 50\%$ curve for the new regression is almost the same as that for the Cao et al. (2013) regression. However, the addition of new lique-faction points has pulled the new $P_L = 85\%$ curve to the right while the addition of no-liquefaction data points has pulled the new $P_L = 15\%$ curve to the left, relative to the original curves, and steepened the slopes of the curves. Overall, the spread between the triggering curves for various probabilities of liquefaction is substantially reduced for the new triggering curves relative to the Cao et al. (2013) curves. The increased number of data points reduces the uncertainty that develops when an individual data point plots in an unexpected position. Furthermore, the addition of data points where liquefaction did not occur has helped constrain the triggering curves on the no-liquefaction side in critical locations.

Summary and Conclusion

In this study, probabilistic liquefaction triggering curves for gravelly soils based on the Dynamic Penetration Test (DPT) have been developed and can be used for liquefaction evaluation of gravelly soils for a range of earthquake magnitudes, tectonic settings, and geologic environments. These curves are a significant step forward compared to those developed by Cao et al. (2013) because they are based on 190% more data points and ten earthquakes instead of one. DPT soundings were conducted at locations around the world where liquefaction or no-liquefaction case histories of gravelly soils were observed during earthquake events in the past. The expanded data set consists of 137 data points (80 liquefactions and 57

no-liquefaction) from seven different countries during 10 different earthquakes in a variety of depositional environments.

As a part of this study, we have used the expanded collection of gravel case history data points to develop a new set of probabilistic liquefaction triggering curves with logistic regression analysis. The logistic regression has been performed to formulate the probability of liquefaction as a function of DPT blow count (N'_{120}) , cyclic stress ratio (CSR), and earthquake moment magnitude (M_w) .

Because of the larger number of data points, particularly at critical locations, the new triggering curves are better constrained by data relative to the Cao et al. (2013) curves. For example, liquefaction and no-liquefaction case histories for ports in Greece and New Zealand constrained the new triggering curves to shift upward for N'_{120} values less than about 10 compared to the Cao et al. (2013) curves, indicating higher cyclic resistance ratios. Likewise, the combination of liquefaction and no-liquefaction data points at higher N'_{120} and CSR values pulled the new $P_L = 15\%$ curve to the left and the new $P_L = 85\%$ curve to the right, relative to these curves, and steepened the slopes of the new curves. This narrowing of the differences between the probabilistic triggering curves indicates a reduction in uncertainty in obtaining the liquefaction potential of gravelly soils.

The results from the regression analysis have also been used to develop a new magnitude scaling factor (MSF) equation exclusively for gravelly soil. The new MSF curve plots about midway between the original Seed and Idriss (1982) curve and the lower-bound NCEER/NSF curve (Youd and Idriss 2001). In addition, this curve is almost identical to the Idriss and Boulanger (2008) MSF curve for sand, which indicates that the effect of magnitude on liquefaction resistance is similar for both sands and sandy gravels.

The DPT triggering curves from this study are not calibrated for assessing the liquefaction of sand or silty sand profiles. They are

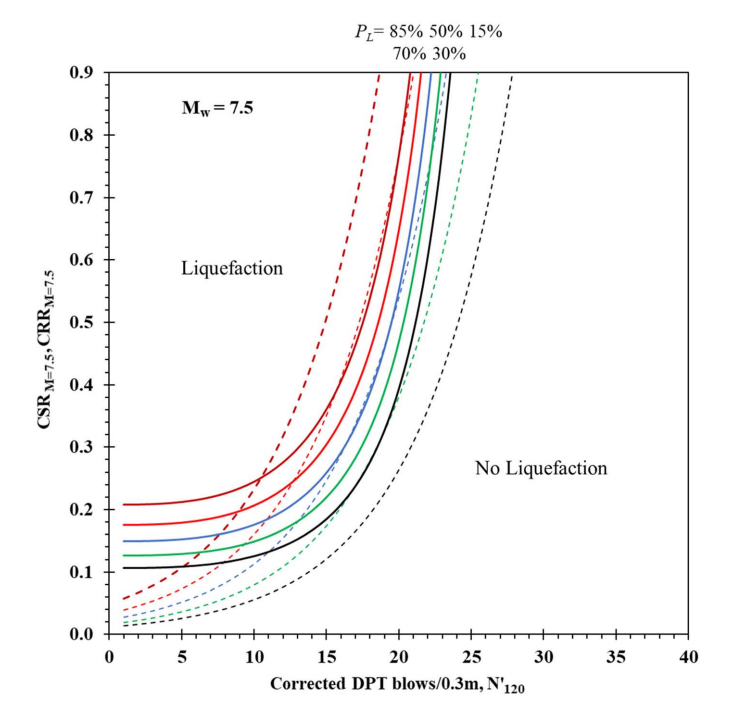


Fig. 11. Probabilistic liquefaction triggering curves from this study (solid lines) relative to triggering curves originally proposed by Cao et al. (2013) (dashed lines).

intended for use when the gravel size and percentage are judged to present a problem for liquefaction assessment with SPT- or CPT-based approaches. Although this DPT based triggering procedure provides a suitable alternative to the BPT- and SPT- or CPT-based procedures for directly evaluating the liquefaction potential of gravelly soil, the effect of relatively large particles on the DPT resistance is still not clearly identified. Additional work is required on the size and percentage of gravel which might artificially increase the penetration resistance. In addition, more quantitative documentation is needed on the effect of side friction on the penetration resistance. The information regarding the energy loss during penetration would further improve the correlation between the energy corrected DPT blow count and the liquefaction resistance of gravelly deposits.

Data Availability Statement

Some or all data, models, or code that support the findings of this study are available from the corresponding author upon reasonable request. These data include electronic versions of the gravel liquefaction database listed in Table S1.

Acknowledgments

Funding for this study was provided by Grant No. G16AP00108 from the US Geological Survey Earthquake Hazard Reduction Program, Grant Nos. CMMI-1663288 and CMMI-1663546 from the National Science Foundation, and National Natural Science Foundation of China Grant No. 51968015. This funding is gratefully acknowledged. However, the opinions, conclusions, and recommendations in this paper do not necessarily represent those of the sponsors. We are grateful to Gerhart-Cole, Inc. for donating the PDA equipment used in this study. We also express sincere appreciation to Tiffany Krall, Professor Misko Cubrinovski, and Rick Wentz for arranging access for DPT testing at Centreport in

Wellington, New Zealand; to David Hemstreet and Tim Weiss at the Alaska DOT for providing drilling equipment and access to sites for DPT testing in Alaska; Professor Kevin Franke and Donald Anderson for arranging a DPT test in Japan; Luca Minerelli for help in arranging access for DPT testing at sites in Italy; and to Professor George Athanasopoulos for arranging access for DPT testing at sites in Cephalonia, Greece.

Supplemental Materials

Table S1 is available online in the ASCE Library (www.ascelibrary.org).

References

- Andrus, R. D. 1994. "In situ characterization of gravelly soils that liquefied in the 1983 Borah Peak earthquake." Ph.D. dissertation, Civil Engineering Dept., Univ. of Texas at Austin.
- Andrus, R. D., and K. H. Stokoe. 1997. Liquefaction resistance based on shear wave velocity: Report to the NCEER workshop on evaluation of liquefaction resistance (9/18/97 version). Buffalo, NY: National Center for Earthquake Engineering Research.
- ASTM. 2018. Standard test method for use of the dynamic cone penetrometer in shallow pavement applications. ASTM D6951/D6951M-18. West Conshohocken, PA: ASTM.
- Athanasopoulos-Zekkos, A., D. Zekkos, K. M. Rollins, J. Hubler, J. Higbee, and A. Platis. 2019. "Earthquake performance and characterization of gravel-size earthfills in the ports of Cephalonia, Greece, following the 2014 Earthquakes." In Proc., 7th Int. Conf. on Earthquake Geotechnical Engineering: Earthquake Geotechnical Engineering for Protection and Development of Environment and Constructions, edited by F. Silvestri and N. Moraci, 1212–1219. Rome: Associazione Geotecnica Italiana.
- Baratta, M. 1910. La Catastrofe Sismica Calabro-Messinese (28 dicembre 1908). Roma: Società Geografica Italiana.
- Bardet, J. P., K. O. Cetin, W. Lettis, E. Rathje, G. Rau, R. B. Seed, and D. Ural. 2000. "Chapter 7. Soil liquefaction, landslides and subsidence." *Earthquake Spectra* 16: 141–162.
- Bindi, D., F. Pacor, L. Luzi, R. Puglia, M. Massa, G. Ameri, and R. Paolucci. 2011. "Ground motion prediction equations derived from the Italian strong motion database." *Bull. Earthquake Eng.* 9 (6): 1899–1920
- Boulanger, R. W., and I. M. Idriss. 2014. CPT and SPT based liquefaction triggering procedures. Rep. No. UCD/CGM-14/01. Davis, CA: Univ. of California, Davis.
- Boulanger, R. W., and I. M. Idriss. 2015. "CPT-based liquefaction triggering procedure." *J. Geotech. Geoenviron. Eng.* 142 (2): 04015065. https://doi.org/10.1061/(ASCE)GT.1943-5606.0001388.
- BSI (British Standard Institution). 2012. Geotechnical investigation and testing: Field testing: Part 2: Dynamic probing. BS EN ISO 22476-2:2005+A1:2011. London: BSI.
- Cao, Z., K. M. Rollins, X. Yuan, T. L. Youd, M. Talbot, J. Roy, and S. Amoroso. 2019. "Applicability and reliability of CYY formula based on Chinese dynamic penetration test for liquefaction evaluation of gravelly soils." *Chin. J. Geotech. Eng.* 41 (9): 1628–1635. https://doi.org/10.11779/CJGE201601018.
- Cao, Z., T. L. Youd, and X. Yuan. 2011. "Gravelly soils that liquefied during 2008 Wenchuan, China Earthquake, Ms = 8.0." Soil Dyn. Earthquake Eng. 31 (8): 1132–1143. https://doi.org/10.1016/j.soildyn.2011 .04.001.
- Cao, Z., T. L. Youd, and X. Yuan. 2013. "Chinese dynamic penetration test for liquefaction evaluation in gravelly soils." *J. Geotech. Geoenviron. Eng.* 139 (8): 1320–1333. https://doi.org/10.1061/(ASCE)GT.1943-5606 .0000857.
- Cao, Z., X. Yuan, T. L. Youd, and K. M. Rollins. 2012. "Chinese dynamic penetration tests (DPT) at liquefaction sites following 2008 Wenchuan Earthquake." In *Proc.*, 4th Int. Conf. on Geotechnical and Geophysical Site Characterization, 1499–1504. London: Taylor & Francis.

- Chen, L., X. Yuan, Z. Cao, R. Sun, W. Wang, and H. Liu. 2018. "Characteristics and triggering conditions for naturally deposited gravelly soils that liquefied following the 2008 Wenchuan Mw 7.9 earthquake, China." *Earthquake Spectra* 34 (3): 1091–1111.
- Chinese Design Code. 2001. *Design code for building foundation of Chengdu region*. [In Chinese.] DB51/T5026-2001. Chengdu, China: Administration of Quality and Technology.
- Chu, B. L., S. C. Hsu, S. E. Lai, and M. J. Chang. 2000. Soil liquefaction potential assessment of the Wufeng Area after the 921 Chi-Chi earthquake. [In Chinese.] Rep. of National Science Council. Taipei, Taiwan: National Research Council of Taiwan.
- Coulter, H. W., and R. R. Migliaccio. 1966. Effect of the Earthquake of March 22, 1964 at Valdez, Alaska. U.S. Geological Survey Professional Paper 542-C. Washington, DC: USGS.
- Cubrinovski, M., J. Bray, C. de la Torre, M. Olsen, B. Bradley, G. Chiaro, E. Stocks, and L. Wotherspoon. 2017. "Liquefaction effects and associated damages observed at the Wellington CentrePort from the 2016 Kaikōura earthquake." *Bull. N.Z. Soc. Earthquake Eng.* 50 (2): 152–173. https://doi.org/10.5459/bnzsee.50.2.152-173.
- Cubrinovski, M., J. D. Bray, C. Christopher de la Torre, M. Olsen, B. Bradley, G. Chiaro, E. Stocks, L. Wotherspoon, and T. Krall. 2018. "Liquefaction-induced damage and CPT characterization of the reclamations at CentrePort, Wellington." *Bull. Seismol. Soc. Am.* 108 (3B): 1695–1708. https://doi.org/10.1785/0120170246.
- Daniel, C. R., J. A. Howie, and A. Sy. 2003. "A method for correlating large penetration test (LPT) to standard penetration test (SPT) blow counts." *Can. Geotech. J.* 40 (1): 66–77. https://doi.org/10.1139/t02-094.
- DeJong, J. T., M. Ghafghazi, A. P. Sturm, D. W. Wilson, J. den Dulk, R. J. Armstrong, A. Perez, and C. A. Davis. 2017. "Instrumented Becker penetration test. I: Equipment, operation, and performance." *J. Geotech. Geoenviron. Eng.* 143 (9): 04017062. https://doi.org/10.1061/(ASCE) GT.1943-5606.0001717.
- DeJong, J. T., A. P. Sturm, and M. Ghafghazi. 2016. "Characterization of gravelly alluvium." *Soil Dyn. Earthquake Eng.* 91 (Dec): 104–115. https://doi.org/10.1016/j.soildyn.2016.09.032.
- Dhakal, R., M. Cubrinovski, J. Bray, and C. de la Torre. 2020. "Liquefaction assessment of reclaimed land at Centreport, Wellington." *Bull. N.Z. Soc. Earthquake Eng.* 53 (1): 1–12. https://doi.org/10.5459/bnzsee.53.1.1-12.
- Dhakal, R., M. Cubrinovski, C. de la Torre, and J. Bray. 2019. "Site characterization for liquefaction assessment of gravelly reclamations at CentrePort, Wellington." In Vol. 20 of *Proc., 7th Int. Conf. on Earthquake Geotechnical Engineering*, edited by F. Silvestri and N. Moraci, 2102–2110. Rome: Italian Geotechnical Association.
- Franke, K. W., and K. M. Rollins. 2017. "Lateral spread displacement and bridge foundation case histories from the 1991 M7.6 Earthquake near Limón, Costa Rica." *J. Geotech. Geoenviron. Eng.* 143 (6): 05017002. https://doi.org/10.1061/(ASCE)GT.1943-5606.0001653.
- Ghafghazi, M., J. T. DeJong, A. P. Sturm, and C. E. Temple. 2017. "Instrumented Becker penetration test. II: iBPT-SPT correlation for characterization and liquefaction assessment of gravelly soils." *J. Geotech. Geoenviron. Eng.* 143 (9): 04017063. https://doi.org/10.1061/(ASCE) GT.1943-5606.0001718.
- Gibbs, H. J., and W. C. Holtz. 1957. "Research on determing the density of sands by spoon penetration testing." In Vol. 1 of *Proc.*, 4th Int. Conf. Soil Mechanics and Foundation Engineering, 35. New York: LexisNexis.
- Golesorkhi, R. 1989. "Factors influencing the computation determination of earthquake-induced shear stresses in sandy soils." Ph.D. dissertation, Civil Engineering Dept., Univ. of California-Berkeley.
- Harder, L. F., and H. B. Seed. 1986. Determination of penetration resistance for coarse-grained soils using the Becker hammer drill. Rep. No. UCB/EERC-86/06. Berkeley, CA: Earthquake Engineering Research Center, Univ. of California, Berkeley.
- Hazen, A. 1911. "Discussion of 'Dams on Sand Foundations by A.C. Koenig'." Trans. ASCE 73 (11): 199–203.
- Hubler, J., A. Athanasopoulos-Zekkos, and D. Zekkos. 2017. "Monotonic, cyclic and post-cyclic simple shear response of three uniform gravels in constant volume conditions." *J. Geotech. Geoenviron. Eng.* 143 (9): 04017043. https://doi.org/10.1061/(ASCE)GT.1943-5606.0001723.

- Hubler, J., A. Athanasopoulos-Zekkos, and D. Zekkos. 2018. "Monotonic and cyclic simple shear response of gravel-sand mixtures." *Soil Dyn. Earthquake Eng.* 115 (Dec): 291–304. https://doi.org/10.1016/j.soildyn.2018.07.016.
- Idriss, I. M. 1999. "An update to the Seed-Idriss simplified procedure for evaluating liquefaction potential." In Proc., TRB Workshop on New Approaches to Liquefaction, Publication No. FHWA-RD-99-165. Washington, DC: Federal Highway Administration.
- Idriss, I. M., and R. W. Boulanger. 2008. Soil liquefaction during earth-quakes. Oakland, CA: Earthquake Engineering Research Institute.
- Ishihara, K. 1985. "Stability of natural deposits during earthquakes." In Vol. 1 of *Proc.*, 11th Int. Conf. on Soil Mech. and Found. Eng., 321–376. Rotterdam, Netherlands: Balkema.
- Kayen, R., R. E. S. Moss, E. M. Thompson, R. B. Seed, K. O. Cetin, A. D. Kiureghian, Y. Tanaka, and K. Tokimatsu. 2013. "Shear-wave velocity-based probabilistic and deterministic assessment of seismic soil lique-faction potential." *J. Geotech. Geoenviron. Eng.* 139 (3): 407–419. https://doi.org/10.1061/(ASCE)GT.1943-5606.0000743.
- Kociu, S. 2004. "Induced seismic impacts observed in coast area of Albania: Case studies." In *Proc.*, 5th Int. Conf. on Case Histories in Geotechnical Engineering. Rolla, MO: Missouri Univ. of Science and Technology.
- Kokusho, T., Y. Tanaka, K. Kudo, and T. Kawai. 1995. "Liquefaction case study of volcanic gravel layer during 1993 Hokkaido-Nansei-Oki earthquake." In Proc. 3rd Int. Conf. on Recent Advances on Soil Dynamics and Geotechnical Earthquake Engineering (St. Louis), 235–242. Rolla, MO: Missouri Univ. of Science and Technology.
- Kokusho, T., and Y. Yoshida. 1997. "SPT N-value and S-wave velocity for gravelly soils with different grain size distribution." Soils Found. 37 (4): 105–113. https://doi.org/10.3208/sandf.37.4_105.
- Liao, S., and R. V. Whitman. 1986. "Overburden correction factors for SPT in sand." *J. Geotech. Eng.* 112 (3): 373–377. https://doi.org/10.1061/(ASCE)0733-9410(1986)112:3(373).
- Liao, S. S. C., D. Veneziano, and R. V. Whitman. 1988. "Regression models for evaluating liquefaction probability." *J. Geotech. Geoenviron. Eng.* 114 (4): 389–411. https://doi.org/10.1061/(ASCE)0733-9410(1988) 114:4(389).
- Lin, P., C. Chang, and W. Chang. 2004. "Characterization of liquefaction resistance in gravelly soil: Large hammer penetration test and shear wave velocity approach." Soil Dyn. Earthquake Eng. 24 (9–10): 675–687. https://doi.org/10.1016/j.soildyn.2004.06.010.
- Lopez, S., X. Vera-Grunauer, K. Rollins, and G. Salvatierra. 2018. "Gravelly soil liquefaction after the 2016 Ecuador earthquake." In *Proc.*, Conf. on Geotechnical Earthquake Engineering and Soil Dynamics V, 273–285. Reston, VA: ASCE.
- Maurenbrecher, P. M., A. Den Outer, and H. J. Luger. 1995. "Review of geotechnical investigations resulting from the Roermond April 13, 1992 earthquake." In *Proc.*, 3rd Int. Conf. on Recent Advances in Geotechnical Earthquake Engineering and Soil Dynamics, 645–652. Rolla, MO: Missouri Univ. of Science and Technology.
- McCulloch, D. S., and M. G. Bonilla. 1970. Effects of the earthquake of March 27, 1964, on the Alaska Railroad. Washington, DC: US Government Printing Office.
- Morales, C., C. Ledezma, E. Saez, S. Boldrini, and K. M. Rollins. 2020. "Seismic failure of an old pier during the 2014 M_w 8.2, Pisagua, Chile earthquake." *Earthquake Spectra* 36 (2): 880–903. https://doi.org/10.1177/8755293019891726.
- Nikolaou, S., D. Zekkos, D. Assimaki, and R. Gilsanz. 2014. "GEER/EERI/ATC Earthquake Reconnaissance January 26th/February 2nd 2014 Cephalonia, Greece Events, Version 1." Accessed August 5, 2021. https://www.geerassociation.org/index.php/component/geer_reports /?view=geerreports&id=32.
- Pavlides, S., Y. Muceku, A. Chatzipetrow, G. Georgious, I. Lazos, A. Beqiraj, and H. Reçi. 2020. Preliminary report on the ground effects of the November 26, 2019, Albania earthquake Thessaloniki, Greece: Earthquake Geology Research Team, Dept. of Geology, Aristotle Univ. of Thessaloniki.
- Rinehart, R., A. Brusak, and N. Potter. 2016. *Liquefaction triggering assessment of gravelly soils: State-of-the-Art Review.* Rep. ST-2016-0712-01. Washington, DC: US Bureau of Reclamation.

- Rollins, K. M., S. Amoroso, G. Milan, L. Minerelli, M. Vassallo, and G. Di Giulio. 2020. "Gravel liquefaction assessment using the dynamic cone penetration test based on field performance from the 1976 Friuli earthquake." J. Geotech. Geoenviron. Eng. 146 (6): 04020038. https://doi .org/10.1061/(ASCE)GT.1943-5606.0002252.
- Rollins, K. M., C. Ledezma, and G. Montalva, A. Becerra, G. Candia, D. Jara, K. Franke, and E. Saez. 2014. Geotechnical Aspects of April 1, 2014, M8.2 Iquique, Chile Earthquake. GEER Association Rep. No. GEER-038. Atlanta: Georgia Tech Univ.
- Rollins, K. M., M. W. Talbot, K. W. Franke, and S. Amoroso. 2018. Evaluation and optimization of dynamic cone penetration test (DPT) for deterministic and performance-based assessment of liquefaction in gravel. Final Report on Grant No. G16AP00108. Washington, DC: US Geological Survey, External Research Program.
- Seed, H. B., and I. M. Idriss. 1971. "Simplified procedure for evaluating soil liquefaction potential." J. Soil Mech. Found. Div. 97 (9): 1249–1273. https://doi.org/10.1061/JSFEAQ.0001662.
- Seed, H. B., and I. M. Idriss. 1982. Ground motions and soil liquefaction during earthquakes. Monograph Series. Berkeley, CA: Earthquake Engineering Research Institute, Univ. of California, Berkeley.
- Seed, H. B., J. Lysmer, and P. P. Martin. 1976. "Pore-water pressure changes during soil liquefaction." *J. Geotech. Eng.* 102 (4): 323–346.
- Seed, H. B., K. Tokimatsu, L. F. Harder, and R. M. Chung. 1985. "Influence of SPT procedures in soil liquefaction resistance evaluations." *J. Geotech. Eng.* 111 (12): 1425–1445. https://doi.org/10.1061/(ASCE)0733 -9410(1985)111:12(1425).
- Seed, R. B., et al. 2003. "Recent advances in soil liquefaction engineering: A unified and consistent framework." In Proc., 26th Annual ASCE Los Angeles Geotechnical Spring Seminar, Earthquake Engineering Research Center, Univ. of California, Berkeley.
- She, K., D. P. D. P. Horn, and P. Canning. 2006. "Porosity and hydraulic conductivity of mixed sand-gravel sediment." In *Proc.*, 41st Defra Conf. on Flood and Coastal Risk Management, 16. Wallingford, UK: Hydraulics Research Station.
- Sirovich, L. 1996a. "In-situ testing of repeatedly liquefied gravels and liquefied overconsolidated sands." Soils Found. 36 (4): 35–44. https:// doi.org/10.3208/sandf.36.4_35.
- Sirovich, L. 1996b. "Repetitive liquefaction at gravelly site and liquefaction in overconsolidated sands." Soils Found. 36 (4): 23–34. https://doi.org /10.3208/sandf.36.4_23.
- Sy, A. 1997. "Twentieth Canadian geotechnical colloquium: Recent developments in the Becker penetration test: 1986–1996." Can. Geotech. J. 34 (6): 952–973. https://doi.org/10.1139/t97-066.

- Talbot, M. A. 2018. Dynamic cone penetration test for liquefaction evaluation of gravelly soils." Ph.D. dissertation, Civil and Environmental Engineering Dept., Brigham Young Univ.
- Tatsuoka, F., J. Koseki, and A. Takahashi. 2017. "Earthquake-induced damage to earth structures and proposal for revision of their design policy—Based on a case history of the 2011 off the Pacific coast of Tohoku earthquake." *J. JSCE* 5 (1): 101–112. https://doi.org/10.2208/journalofjsce.5.1_101.
- Tokimatsu, K., and Y. Yoshimi. 1983. "Empirical correlation of soil lique-faction based on SPT N-value and fines content." *Soils Found.* 23 (4): 56–74. https://doi.org/10.3208/sandf1972.23.4_56.
- Wang, W. S. 1984. "Earthquake damages to earth dams and levees in relation to soil liquefaction and weakness in soft clays." In *Proc., Int. Conf. Case Histories Geotech. Eng.*, 511–521. Rolla, MO: Missouri Univ. of Science and Technology.
- Worden, C. B., D. J. Wald, T. I. Allen, K. Lin, and G. Cua. 2010. "Integration of macroseismic and strong-motion earthquake data in ShakeMap for real-time and historic earthquake analysis." Accessed August 5, 2021. http://earthquake.usgs.gov/earthquakes/shakemap/.
- Yegian, M. K., V. G. Ghahraman, and R. N. Harutiunyan. 1994. "Liquefaction and embankment failure case histories, 1988 Armenia earthquake." J. Geotech. Eng. 120 (3): 581–596. https://doi.org/10.1061/(ASCE)0733-9410(1994)120:3(581).
- Youd, T. L., et al. 2001. "Liquefaction resistance of soils: Summary report from the 1996 NCEER and 1998 NCEER/NSF workshops on evaluation of liquefaction resistance of soils." *J. Geotech. Geoenviron. Eng.* 127 (10). https://doi.org/10.1061/(ASCE)1090-0241(2001)127:10(817).
- Youd, T. L., E. L. Harp, D. K. Keefer, and R. C. Wilson. 1985. "The Borah Peak, Idaho Earthquake of October 29, 1983-Liquefaction." *Earthquake Spectra* 2 (1): 71–89. https://doi.org/10.1193/1.1585303.
- Youd, T. L., and S. N. Hoose. 1978. *Historic ground failures in Northern California triggered by earthquakes*. Washington, DC: United States Government Printing Office.
- Youd, T. L., and I. M. Idriss. 2001. "Liquefaction resistance of soils: Summary report from the 1996 NCEER and 1998 NCEER/NSF workshops on evaluation of liquefaction resistance of soils." J. Geotech. Geoenviron. Eng. 127 (4): 297–313. https://doi.org/10.1061/(ASCE)1090-0241 (2001)127:4(297).
- Youd, T. L., and S. K. Noble. 1997. "Liquefaction criteria based on statistical and probabilistic analyses." In Vol. 22 of *Proc.*, *NCEER Workshop on Evaluation of Liquefaction Resistance of Soils*, *NCEER Technical Rep. No: NCEER-97*, 201–205. Buffalo, NY: National Center for Earthquake Engineering Research.